Impact of Mesh Resolution on Re-Entry Patterns in Healing Infarction using a Biventricular Digital Twin Model

Lucas Arantes Berg[1], Hector Martinez-Navarro[2], Ruben Doste[1], Blanca Rodriguez[1]

[1] University of Oxford, Oxford, United Kingdom
[2] Universitat de Valencia, Valencia, Spain

Abstract

Mesh resolution is a critical component in the development of cardiac digital twin models designed to replicate patient-specific electrophysiological behaviour. This parameter not only affects simulation performance, but also plays a pivotal role in accurately capturing arrhythmogenic mechanisms, such as ventricular re-entry, which is a key feature of life-threatening arrhythmias in heart diseases. In this study, we explore how different mesh resolutions influence the formation and stability of re-entry circuits using an healing infarcted region. Simulations are performed on a human-based biventricular model that includes a Purkinje network and an infarcted region with ionic remodeling by employing a high-performance GPU-based cardiac solver. Notably, we find that even when conduction velocities are adjusted to match across resolutions, the resulting re-entry onset differ, occurring around $4340\ ms$*,* $3640\ ms$ *and* $5080\ ms$*, for* $250\ \mu m$*,* $300\ \mu m$ *and* $350\ \mu m$ *mesh resolutions, respectively. Execution times were* $46.72\ hrs$*,* $26.95\ hrs$ *and* $16.06\ hrs$*. These findings suggest the importance of mesh resolution choice in digital twin applications, particularly for arrhythmia risk assessment and personalized therapy planning that consider the Purkinje network.*

1. Introduction

Cardiac digital twin models aim to replicate patient-specific electrophysiological behavior and have shown promise for personalized therapy, clinical decision support, and understanding life-threatening conditions such as cardiomyopathies and ventricular tachycardia (VT) [1]. Their development, however, is computationally demanding and requires careful calibration of multiple parameters to match clinical data.

Among these, biventricular mesh resolution and tissue conduction velocity (CV) are particularly important, especially when modeling slow-conducting diseased tissue [2] and the Purkinje network [3]. These choices must balance electrophysiological accuracy with feasible runtimes for arrhythmic risk simulations [4].

In this work, we investigate how mesh resolution and Purkinje–myocardium coupling affect VT dynamics in a human biventricular model with a healing infarcted region. Tissue conductivities were calibrated using an automatic parameterization strategy [5] to ensure consistent CVs across resolutions.

2. Methods

2.1. Clinical data and computational mesh

We used a human biventricular MRI-derived mesh [6], previously applied for ECG personalization [7–9], coupled with a Purkinje network (Figure 1A).

To assess mesh resolution effects, three discretizations were tested for the biventricular mesh: $250\ \mu m$ ($6,845,153$ control volumes), $300\ \mu m$ ($3,961,167$) and $350\ \mu m$ ($2,494,526$). The Purkinje mesh was fixed at $100\ \mu m$ (36,176). These resolution values are based on previous works [2, 10, 11].

A healing infarct was introduced in the anteroseptal region to represent left anterior descending artery occlusion (Figure 1B). The infarct was modeled as a $25\ mm$ radius sphere, surrounded by a $4\ mm$ border zone [12].

2.2. Monodomain model

Electrical propagation through cardiac tissue was described by the monodomain model due to its lower computational cost compared to the bidomain model. The mathematical model for the myocardium and Purkinje system, along with their coupling, is given following the finite volume formulation presented in [13].

The Purkinje-Muscle-Junction (PMJ) coupling is modelled by a fixed resistance, linking a Purkinje element to several myocardium elements. Therefore, an additional flux J_{PMJ} ($\mu A/cm^2$) using a fixed resistance R_{PMJ} and by coupling a single Purkinje control volume to its N_{PMJ} closest myocardium control volumes. Moreover, the PMJ flux is given as a non-homogeneous Neumann boundary condition by:

$$J_{PMJ} = \frac{1}{h_P^2} \sum_{k=1}^{N_{PMJ}} \frac{(V_P - V_{M_k})}{R_{PMJ}}, \quad (1)$$

where the sign of the flux determines if J_{PMJ} exerts its action in the anterograde or retrograde direction.

To numerically solve the monodomain model, the GPU-based cardiac solver MONOALG3D [13,14] was used with a time discretization equal to $dt = 0.01\ ms$ for the associated PDE and ODE system. Purkinje coupling parameters are fixed across resolutions with values of $R_{PMJ} = 500\ M\Omega$ and $N_{PMJ} = 60$.

An approximation for the ECG was computed by assuming that the tissue is immersed in an unbounded volume conductor and using the formulation described in [13, 14].

2.3. Cellular models

To model the cellular dynamics of the myocardium domain we utilized a modified version of the human-based ToR-ORd [15], while for the Purkinje cells the human-based Trovato model [16]. Modifications on the ToR-ORd model are summarised in Table 1 and reproduce a steeper APD restitution curve that promotes spiral break up and hence ventricular fibrillation (VF) in the model, as in [17]. Healing infarction conditions (few weeks post coronary occlusion) were reproduced through ionic alterations in the ToR-ORd model using the parameters presented in the work from Riebel et al [18].

2.4. Stimulus protocol

Sinus rhythm was simulated by delivering an initial stimulus at the His-bundle and considering an arrhythmic pacing protocol with a decreasing cycle length (CL) based on the work from Sayers et al. [12]. Two beats of $CL = 500\ ms$, followed by two beats of $CL = 450\ ms$, two beats of $CL = 425\ ms$, two beats of $CL = 400\ ms$, two beats of $CL = 375\ ms$ and three beats of $CL = 350ms$. After the last stimulus, we wait for a sustained ventricular arrhythmia activity. Total simulation time is equal to $t_{max} = 6500ms$.

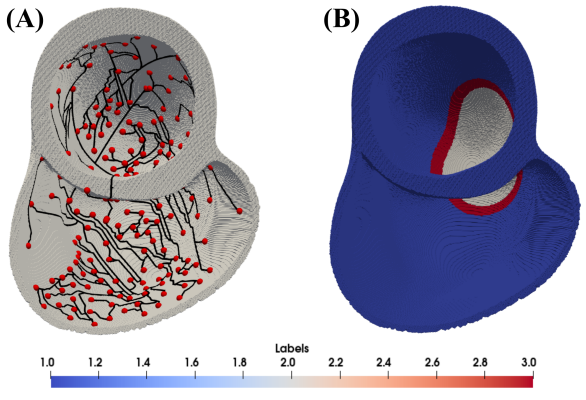

Figure 1: Biventricular mesh (350 μm) used for the computational simulations with its coupled Purkinje network (A) and healing infarcted region (B). Regions highlighted in blue (healthy), red (borderzone) and white (infarct).

Parameter	Value	Parameter	Value
I_{CaL}	0.60	I_{Nab}	1.31
I_{Na}	1.39	I_{Cab}	1.36
I_{to}	1.48	I_{pCa}	1.10
I_{NaL}	1.39	I_{CaCl}	0.74
I_{Kr}	1.13	I_{Clb}	0.68
I_{Ks}	0.82	J_{rel}	0.62
I_{K1}	0.75	J_{up}	1.37
I_{Kb}	0.91	$inact_{I_{CaL}}$	1.90
I_{NaCa}	0.91	$inact_{I_{Na}}$	0.50
I_{NaK}	1.28	$inact_{NaL}$	0.66
		$inact_{IKrVar8}$	0.35

Table 1: Ventricular fibrillation scaling factors for the *ToR-ORd* cellular model.

2.5. Conduction velocity

To calibrate the monodomain tissue conductivities across the three space discretizations for the biventricular mesh, the automatic parametrization strategy proposed by Costa et al. [5] (*tuneCV*) was implemented in MONOALG3D setting the stop criterion for the iterative procedure equal to 10^{-3}. A cable of length 12.6 cm was used for CV calibration simulations, with the CV calculated at the middle of the cable considering the local activation time (LAT) as the time when the transmembrane potential of a control volume exceeds a threshold of $-50\ mV$. Conduction velocities for the healthy tissue are given by 65 cm/s (longitudinal), 38 cm/s (transversal) and 47 cm/s (normal), while for healing infarcted tissue these values are 19 cm/s (longitudinal), 12 cm/s (transversal) and 15 cm/s (normal). For the Purkinje network a conductivity of $\sigma_p = 2.25\ S/m$ was calibrated for a CV of 3 m/s using the same procedure. All values of CVs are based on previous works [8, 18]. Table 2 summarizes the calibrated conductivities for each cell type across the different space discretizations.

	250 μm		300 μm		350 μm	
{S/m}	HZ	IZ	HZ	IZ	HZ	IZ
σ_l	0.2371	0.0823	0.2502	0.0906	0.2698	0.1006
σ_t	0.1007	0.0421	0.1126	0.0463	0.1208	0.0521
σ_n	0.1381	0.0546	0.1496	0.0600	0.1623	0.0667

Table 2: Calibrated monodomain tissue conductivities using the *tuneCV* implementation in MONOALG3D across the three space discretizations. HZ: healthy and IZ: infarct.

3. Results and discussion

Figure 2 shows the effect that the mesh resolution has on the tissue CVs for healthy and healing infarcted cells. Monodomain tissue conductivities were calibrated with the automatic parameterization strategy [5] implemented in MonoAlg3D. As can be verified in Figure 2A, without a proper tissue conductivity calibration strategy, we could not keep the same CVs across resolutions. In addition, the calibration procedure proves essential when healing infarcted cells are involved, as we start observing propagation blocks when calibrating the transversal direction due to the slow propagation in that direction, as can be verified by the red crosses in Figure 2B.

Figure 3 shows that sustained VT was obtained for all three mesh resolutions. Despite conduction velocity (CV) calibration using the automatic parameterization strategy, the VT onset time varied: $4340ms$ ($250\mu m$), $3640ms$ ($300\mu m$), and $5080ms$ ($350\mu m$) (Fig.3B). Corresponding simulation runtimes were $46.72h$, $26.95h$, and $16.06h$, respectively.

Differences in VT onset may arise from the Purkinje–myocardium coupling implementation. The fixed number of coupled myocardial control volumes (N_{PMJ}) per Purkinje terminal was maintained across resolutions, potentially altering the effective anterograde PMJ delay at different spatial discretizations. These changes can influence local activation times and modify activation patterns within the healing infarcted region, as can be seen in the transmembrane potential maps (Fig. 3A).

Given the established role of the Purkinje network in re-entrant arrhythmogenesis, these findings highlight the need to assess sensitivity to coupling parameters in models coupled to the Purkinje network. Future work could implement a coupling strategy independent of mesh resolution, like for example, connecting each Purkinje terminal to myocardial elements within a fixed volumetric region (spherical or cylindrical) and adjusting R_{PMJ} to maintain consistent PMJ delays across resolutions.

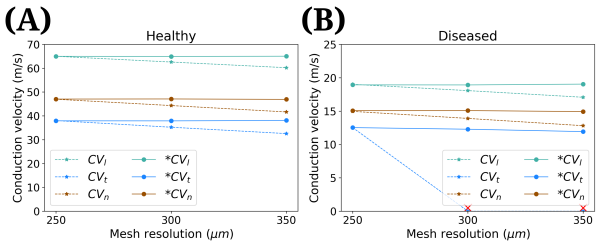

Figure 2: Results for the CV calibration using the automatic parameterization strategy implemented in MonoAlg3D for healthy cells (A) and diseased ones (B). Solid lines are CVs calibrated with the tool ($*CV$), while dashed lines are uncalibrated (CV). Red crosses denote propagation blocks.

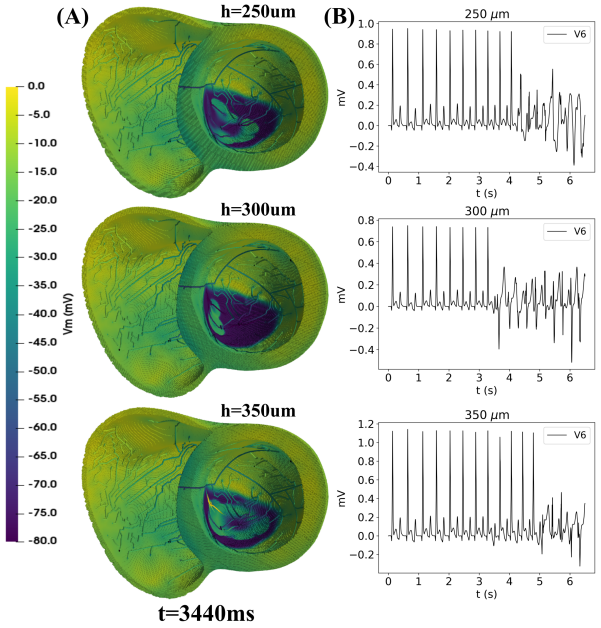

Figure 3: (A) Transmembrane potential at $t = 3440\ ms$ for the three different space discretizations. (B) ECG approximation for lead V6.

4. Conclusion

We presented a study that assesses the effect that mesh resolution has on re-entry patterns, considering an healing infarcted region and Purkinje network coupling. Our results confirmed that calibrating the monodomain tissue conductivity is essential to correctly capture conduction velocities across resolutions, especially when ionic remodeling is considered. Importantly, this study highlights that the usage of a Purkinje coupling implementation that is dependent on the space discretization can affect the activation patterns and change the onset of the VT through the three space discretizations used for the biventricular mesh.

Acknowledgments

This work was funded by a Wellcome Trust fellowship in Basic Biomedical Sciences to B.R. (214290/Z/18/Z), the EPSRC project CompBioMedX (EP/X019446/1), the CompBioMed2 Centre of Excellence in Computational Biomedicine grant agreements No. 675451 and No. 823712. The U.S. Department of Energy's (DOE) Innovative and Novel Computational Impact on Theory and Experiment (INCITE) Program awarded access to Polaris, under contract No. DE-AC02-06CH11357.

References

[1] Qian S, Ugurlu D, Fairweather E, Toso LD, Deng Y, Strocchi M, Cicci L, Jones RE, Zaidi H, Prasad S, et al. Developing cardiac digital twin populations powered by machine

learning provides electrophysiological insights in conduction and repolarization. Nature Cardiovascular Research 2025;4(5):624–636.

[2] Costa CM, Gemmell P, Elliott MK, Whitaker J, Campos FO, Strocchi M, Neic A, Gillette K, Vigmond E, Plank G, et al. Determining anatomical and electrophysiological detail requirements for computational ventricular models of porcine myocardial infarction. Computers in Biology and Medicine 2022;141:105061.

[3] Jabbour RJ, Behradfar E, Debney M, Nygren A, Hartley A, Efimov I, Hocini M, Peters NS, Ng FS, Vigmond EJ. Acute ischaemia and gap junction modulation modify propagation patterns across Purkinje-myocardial junctions. Frontiers in Physiology 2025;16:1540400.

[4] Viola F, Del Corso G, De Paulis R, Verzicco R. GPU accelerated digital twins of the human heart open new routes for cardiovascular research. Scientific Reports 2023; 13(1):8230.

[5] Costa CM, Hoetzl E, Rocha BM, Prassl AJ, Plank G. Automatic parameterization strategy for cardiac electrophysiology simulations. In Computing in Cardiology 2013. IEEE, 2013; 373–376.

[6] Banerjee A, Camps J, Zacur E, Andrews CM, Rudy Y, Choudhury RP, Rodriguez B, Grau V. A completely automated pipeline for 3D reconstruction of human heart from 2D cine magnetic resonance slices. Philosophical Transactions of the Royal Society A 2021;379(2212):20200257.

[7] Camps J, Lawson B, Drovandi C, Minchole A, Wang ZJ, Grau V, Burrage K, Rodriguez B. Inference of ventricular activation properties from non-invasive electrocardiography. Medical Image Analysis 2021;73:102143.

[8] Camps J, Berg LA, Wang ZJ, Sebastian R, Riebel LL, Doste R, Zhou X, Sachetto R, Coleman J, Lawson B, et al. Digital Twinning of the Human Ventricular Activation Sequence to Clinical 12-lead ECGs and Magnetic Resonance Imaging Using Realistic Purkinje Networks for in Silico Clinical Trials. Medical Image Analysis 2024;94:103108.

[9] Camps J, Wang ZJ, Doste R, Berg LA, Holmes M, Lawson B, Tomek J, Burrage K, Bueno-Orovio A, Rodriguez B. Harnessing 12-lead ECG and MRI data to personalise repolarisation profiles in cardiac digital twin models for enhanced virtual drug testing. Medical Image Analysis 2025; 100:103361.

[10] Arevalo HJ, Vadakkumpadan F, Guallar E, Jebb A, Malamas P, Wu KC, Trayanova NA. Arrhythmia risk stratification of patients after myocardial infarction using personalized heart models. Nature Communications 2016; 7(1):11437.

[11] Bishop MJ, Plank G. Stochastic virtual heart model predictions. Nature Cardiovascular Research 2025;1–4.

[12] Sayers JR, Martinez-Navarro H, Sun X, de Villiers C, Sigal S, Weinberger M, Rodriguez CC, Riebel LL, Berg LA, Camps J, et al. Cardiac conduction system regeneration prevents arrhythmias after myocardial infarction. Nature Cardiovascular Research 2025;4(2):163–179.

[13] Berg LA, Oliveira RS, Camps J, Wang ZJ, Doste R, Bueno-Orovio A, dos Santos RW, Rodriguez B. MonoAlg3D: Enabling Cardiac Electrophysiology Digital Twins with an Efficient Open Source Scalable Solver on GPU Clusters. bioRxiv 2025;2025–04.

[14] Sachetto Oliveira R, Martins Rocha B, Burgarelli D, Meira Jr W, Constantinides C, Weber dos Santos R. Performance evaluation of GPU parallelization, space-time adaptive algorithms, and their combination for simulating cardiac electrophysiology. International Journal for Numerical Methods in Biomedical Engineering 2018;34(2):e2913.

[15] Tomek J, Bueno-Orovio A, Passini E, Zhou X, Minchole A, Britton O, Bartolucci C, Severi S, Shrier A, Virag L, et al. Development, calibration, and validation of a novel human ventricular myocyte model in health, disease, and drug block. Elife 2019;8:e48890.

[16] Trovato C, Passini E, Nagy N, Varró A, Abi-Gerges N, Severi S, Rodriguez B. Human Purkinje in silico model enables mechanistic investigations into automaticity and proarrhythmic abnormalities. Journal of Molecular and Cellular Cardiology 2020;142:24–38. ISSN 0022-2828.

[17] Martinez-Navarro H, Bertrand A, Doste R, Smith H, Tomek J, Ristagno G, Oliveira RS, Weber dos Santos R, Pandit SV, Rodriguez B. ECG analysis of ventricular fibrillation dynamics reflects ischaemic progression subject to variability in patient anatomy and electrode location. Frontiers in Cardiovascular Medicine 2024;11:1408822.

[18] Riebel LL, Wang ZJ, Martinez-Navarro H, Trovato C, Camps J, Berg LA, Zhou X, Doste R, Sachetto Oliveira R, Weber dos Santos R, et al. In silico evaluation of cell therapy in acute versus chronic infarction: role of automaticity, heterogeneity and purkinje in human. Scientific Reports 2024;14(1):21584.

Address for correspondence:

Lucas Arantes Berg
University of Oxford, Oxford, United Kingdom
lucas.arantesberg@cs.ox.ac.uk